

Dynamic test evaluation of numerical models for unbonded post-tensioned concrete walls

K.M. Twigden, J. Watkins & R.S. Henry

University of Auckland, Auckland.

S. Sritharan

Iowa State University, Ames, USA.



2013 NZSEE
Conference

ABSTRACT: Post-tensioned precast concrete walls can provide a low-damage seismic resisting system through the use of a controlled rocking mechanism. Seismic analysis of buildings with post-tensioned concrete walls requires accurate estimation of this controlled rocking response. However, only a limited number of laboratory experiments have been conducted to investigate the dynamic response of post-tensioned walls and numerical models have typically been validated against only pseudo-static cyclic test data. Recently conducted cyclic and dynamic tests of single post-tensioned concrete walls have provided a unique opportunity to study existing numerical models. Two types of numerical model were developed to represent the single unbonded post-tensioned concrete wall. A lumped plasticity model was developed using Ruaumoko while a multi-spring macro model was developed using OpenSees. Both models accurately captured the overall cyclic response of the post-tensioned wall specimens, although only the multi-spring macro model explicitly included the uplift and rocking mechanism at the wall base. In addition to the overall responses, comparison of the two models against the dynamic test data focused on the different sources of energy dissipation that occur when the wall rocks. Existing techniques for incorporating the energy dissipation of an unbonded post-tensioned precast concrete wall into numerical models were evaluated. The combination of friction and viscous damping to represent the energy dissipation in an isolated unbonded post-tensioned concrete wall shows promising results.

1 INTRODUCTION

Low-damage structural systems are increasingly being adopted to reduce the economic losses of repair, rebuild, and downtime following an earthquake. Unbonded post-tensioned precast concrete elements are used in many forms of low-damage structural system; one such system consists of a single unbonded post-tensioned precast concrete wall. The use of precast concrete allows for dry connections that accommodate inelastic demand through the opening and closing of an existing joint at the wall base, introducing a rocking mechanism. The unbonded post-tensioning is designed to remain elastic during a design-level earthquake and provides a self-centering restoring force, increasing the stability of the rocking system against overturning. The combination of precast elements and unbonded post-tensioning generates a response that undergoes inelastic deformations with minimal damage. However, due to the minimal damage sustained from a seismic event, post-tensioned precast concrete members have limited energy dissipation compared to a traditional reinforced concrete structure.

The concept of connecting precast concrete elements together with unbonded post-tensioning was investigated extensively during the Precast Seismic Structural Systems (PRESSSS) research program conducted in the 1990's. A jointed wall system was developed during the PRESSSS research program and was tested in a five storey prototype building by Priestley et al. (1999). Following the PRESSSS research program several different rocking wall systems have been developed with a significant focus placed on additional energy dissipating elements (Restrepo & Rahman 2007; Sritharan et al. 2008; Marriott 2009).

Many modelling approaches have been investigated for unbonded post-tensioned rocking wall systems

including lumped plasticity models and multi-spring macro models. A lumped plasticity model relies on the assumption that the main inelastic demand occurs at discrete critical sections. Rotational inelastic springs with appropriate non-linear hysteresis behaviour can be assigned to represent the inelastic behaviour at the rocking interface, while elastic elements are used to represent the structural members (Pampanin et al. 2001; Palermo et al. 2007; Henry 2011). Alternatively, a multi-spring model adopts a series of axial springs to represent the wall-to-foundation interface, with additional springs to represent dampers and post-tensioned tendons. The springs at the wall-to-foundation interface are compression only springs that allow gap opening during rocking. (Pennucci et al. 2009).

Unbonded post-tensioned precast concrete wall systems have been subject to numerous pseudo-static lateral load tests and extensive numerical modelling using nonlinear time history analysis to simulate the response of the systems to earthquake excitation (Kurama et al. 2002; Marriott 2009; Ma 2010; Henry 2011). However, only a limited number of laboratory experiments have been conducted to investigate the dynamic response of post-tensioned wall systems and many of the numerical models remain unvalidated by dynamic tests. Understanding the dynamic behaviour of unbonded post-tensioned wall systems is essential to fully understanding their seismic performance. To be able to achieve an accurate prediction of the structural response a realistic energy dissipation model is essential.

The damping in an unbonded post-tensioned concrete wall system with no additional energy dissipating elements consists of contact damping, friction at unbonded surfaces and inherent viscous damping. Contact damping is the energy loss that occurs during rocking impacts between the wall and the foundation (Ma 2010). These different damping mechanisms are usually lumped together using an Equivalent Viscous Damping (EVD) term. Marriott (2009) specifically included a damping model to account for contact damping during dynamic analysis. From experimental free vibration decay Marriott evaluated contact damping in terms of EVD to be 2.4%. This EVD ratio was found to be proportional to the secant stiffness of the system at maximum displacement (which is the release displacement for free vibration decay). Marriott found that the forces within the damping model for contact damping should be proportional to both velocity and displacement. However the actual proportion of contact energy dissipation attributed to both velocity and displacement was not quantified. Using analytical comparisons with experimental free vibration decay it was found that a 50/50 split captured the response decay well for the particular wall studied.

An investigation is undertaken herein which uses two predictive numerical models of different levels of complexity to evaluate recommendations of energy dissipation for unbonded post-tensioned concrete walls. The results of the different energy dissipation schemes implemented in the two models are evaluated against recently performed free vibration tests.

2 EXPERIMENT OVERVIEW

Twigden et al. (2012) conducted a series of laboratory experiments to investigate the cyclic and dynamic behaviour of unbonded post-tensioned rocking walls without additional energy dissipating elements. Pseudo-static reverse cyclic and snap-back free vibration testing was performed on four precast wall panel ends. The precast concrete wall test specimens were 3 m high, 1 m long and 0.12 m thick. The post-tensioning provided the flexural strength for this reason only minimum longitudinal reinforcement was included to satisfy the requirements of the New Zealand Concrete Standard (2006). Due to the high strains expected in the wall at the toes, each wall panel had specifically designed confinement reinforcement in these regions. The confinement reinforcement was designed using the confined concrete model presented by Mander et al. (1988), using the maximum expected concrete compressive strain calculated from the simplified analysis method developed by Aaleti et al. (2009). Two 40 mm crossbar ducts were cast into each wall to accommodate one 15 mm steel bar each. The pre-stressing bar had a measured yield strength of 900 MPa, an ultimate strength of 1100 MPa, and a modulus of elasticity of 200 GPa. The precast concrete walls had a 28 day compressive strength of 35 MPa based on standard cylinder tests.

The wall panel was placed on top of a foundation that was post-tensioned to a strong floor. A high strength, high flow grout was placed between the wall-to-foundation interface to provide an even

contact surface. A 1237 kg concrete mass block was attached to the top of the wall to provide anchorage for the tendons, seismic mass for the dynamic testing, a loading beam for the actuator to be attached, and an anchorage/platform for the Eccentric Mass Shaker (EMS) which was used in later testing. The EMS weighed an additional 812 kg. Snap back free vibration testing was undertaken using a quick release mechanism that was remotely triggered to release the wall from a specified lateral displacement. The snap back data used in this paper is for 2% drift measured 3.1m above the wall-to-foundation interface.

3 NUMERICAL MODELS

Two predictive numerical models were constructed. The first is a lumped plasticity model which was created using Ruaumoko (Carr 2004). The second is a multi-spring macro model created using OpenSees (Mazzoni et al. 2006).

3.1 Ruaumoko – Lumped plasticity model

A simple multi-linear elastic rotational spring definition, as demonstrated in Figure 1a was used to characterise the non-linear behaviour of the unbonded post-tensioned rocking wall specimen. The definition of the spring is predictive and was based on an simplified analytical procedure proposed by Aaleti et al. (2009). The wall itself was modelled using a beam element of length 3.12 m equal to the loading height of the specimen. Half the mass of the wall and the mass of the loading block were lumped at the node placed at top of the wall, while an additional node was created at 3.8 m for the EMS lumped mass.

3.2 OpenSees – Multi-spring macro model

This predictive numerical model has been adapted from Watkins et al. (2013) for this specific specimen and load conditions. The model, which can be seen in Figure 1b, contains four elements: a bed of truss elements representing the rocking interface, truss elements representing the post-tensioning, an elastic beam element representing the wall panel and a rigid link which connects the EMS to the top of the wall. The truss elements representing the rocking interface are fixed at the base, and connected via rigid links to the base of the elastic beam element. The length of the spring or truss element is calculated from recommendations by Perez et al. (Perez et al. 2007). In the confined toe region two springs are used, one for the confined region and the other for the unconfined cover region.

3.3 Loading

Initially the displacement history of the pseudo-static cyclic test was applied to the models to validate the force displacement behaviour of the model. To investigate different damping schemes, both the lumped plasticity and multi-spring macro models were set up to run dynamic time history analyses to emulate the experimental snap back free vibration test results for 2% drift.

3.4 Cyclic Response Comparison

Prior to conducting dynamic analyses, the force displacement response of the two numerical models was verified against the pseudo-static cyclic test results. A comparison between the lateral force-displacement response from the experimental results and each numerical model is shown Figure 2a. Both the lumped plasticity model and multi-spring macro model adequately capture the backbone of the experimental cyclic response with reasonable accuracy. This also provides a satisfactory validation of the simplified analytical method proposed by Aaleti (2009). A complication of the experimental cyclic test which neither model was able to capture was the tendon anchorage loss that occurred during the test. The lumped plasticity model is very simple and does not have the ability to directly model the tendon stress in contrast to the more complex multi-spring macro model. A comparison of the tendon force versus top lateral displacement for the multi-spring macro model and laboratory experiment is shown in Figure 2b. From this figure it is clear that some prestress loss occurred in the tendon during the test. It is intended that the multi-spring macro model will be developed to include adjustment for the prestress losses in the future. Limited hysteretic energy

dissipation was observed during the experimental cyclic test which neither model was able to capture, perhaps due to the inability of the models to capture the prestress loss at the anchorage.

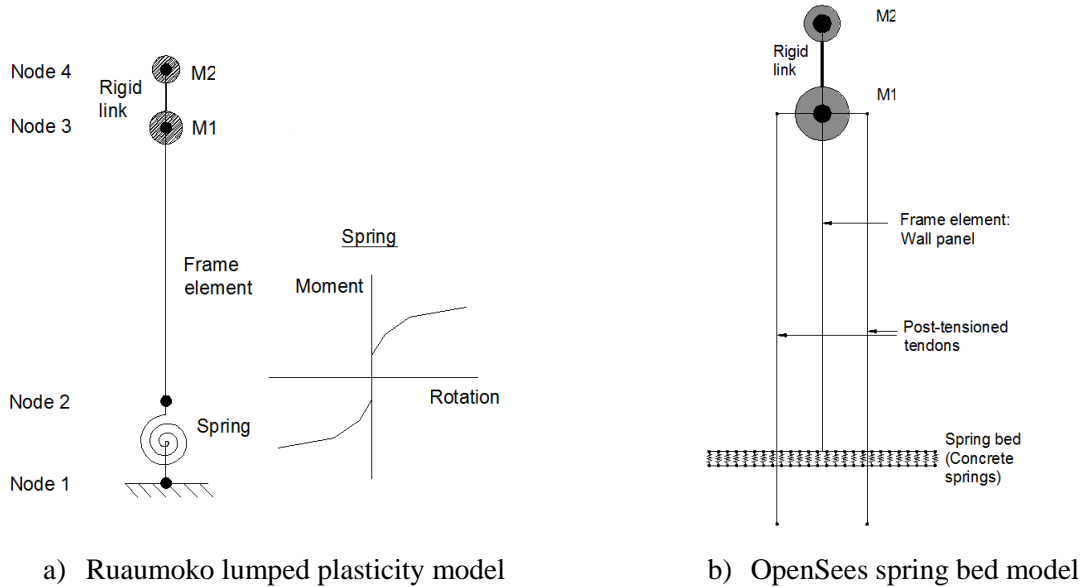


Figure 1: Representations of the SRW models used in Ruaumoko and OpenSees

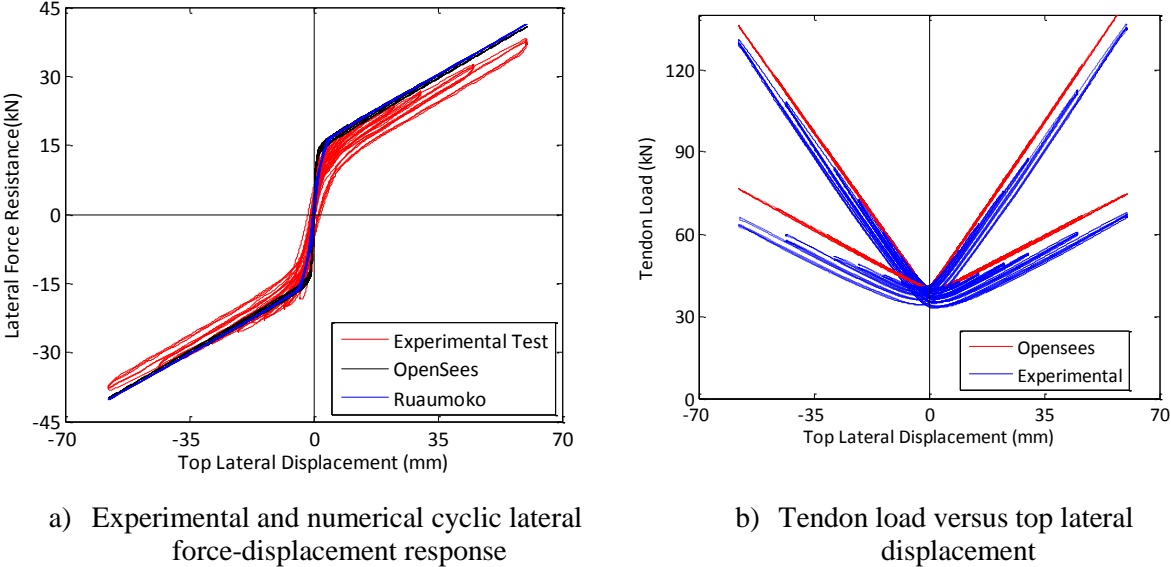


Figure 2: Experimental and numerical comparison of pseudo-static cyclic test

4 DAMPING MODELS

Typically in design the different damping mechanisms associated with a structure are lumped into one parameter; EVD. The total EVD is equal to the sum of elastic and hysteretic damping. The elastic damping in concrete can be attributed to nonlinear behaviour of materials (such as micro-cracking of concrete) and friction. Additionally for an unbonded post-tensioned system the elastic damping is often assumed to account for contact damping as well. Typically 5% elastic damping is assumed for a reinforced concrete building, but buildings with unbonded post-tensioned precast concrete systems are likely to exhibit less damping due to the reduction in cracking. For this reason Henry (2011) used 3% initial stiffness proportional damping and Kurama et al. (2002) used 3% Rayleigh damping applied to the 1st/3rd modes.

Appendix B of the New Zealand Concrete Structures Standard, NZS 3101 (2006), provides recommendations for the seismic design of ductile jointed precast concrete structural systems. When

specifying the EVD of one of the aforementioned systems a lower bound value of 5% damping is recommended when no additional energy dissipating elements are used. In addition to the 5% minimum value of damping, contact damping can also be taken into account. This implies that the EVD ratio for a building with an unbonded post-tensioned wall should be greater than 5% EVD.

To implement the 5% EVD for unbonded post-tensioned wall buildings with no additional energy dissipating elements inferred from Appendix B of NZS 3101 (2006), two Rayleigh damping models were investigated. The first was 5% proportional to the initial stiffness (5% K_i) and the second 5% proportional to the tangent stiffness (5% K_t). Similarly, to follow guidance from Henry (2011) and Kurama et al (2002) 3% initial stiffness (3% K_i) proportional damping and 3% tangent stiffness (3% K_t) damping were executed in the two numerical models described previously. It is important to highlight that the 5% and 3% EVD proportions are intended to apply to a building and not an isolated wall. Although, it is useful to demonstrate the low level of damping for the wall as an isolated component in comparison to values of EVD usually used in analysis for an entire building. The EVD over the first thirty cycles of free vibration response was estimated using the peak-picking method and found to be 2.5%. This supports the 3% EVD which both Kurama et al. (2002) and Henry (2011) used for numerical modelling of entire buildings. The free vibration laboratory test results are compared against the numerical results of both the lumped plasticity model and the multi-spring bed macro model for the same loading in Figure 3 and **Error! Reference source not found.** respectively.

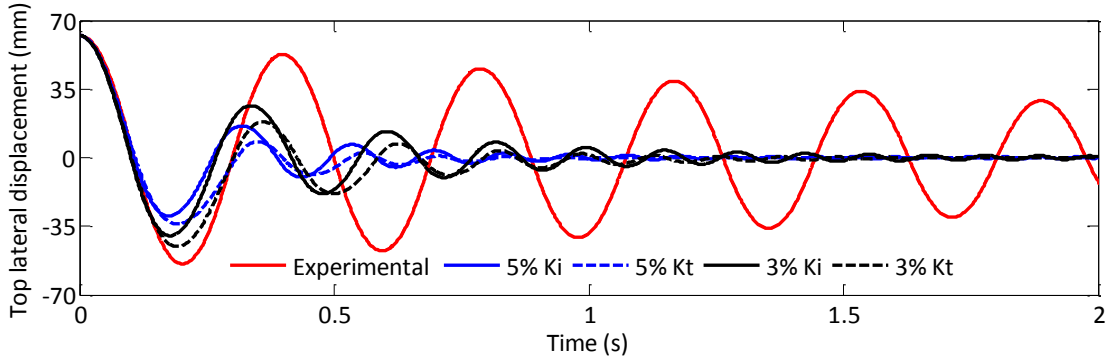


Figure 3: Stiffness proportional damping schemes with the Ruaumoko lumped plasticity model

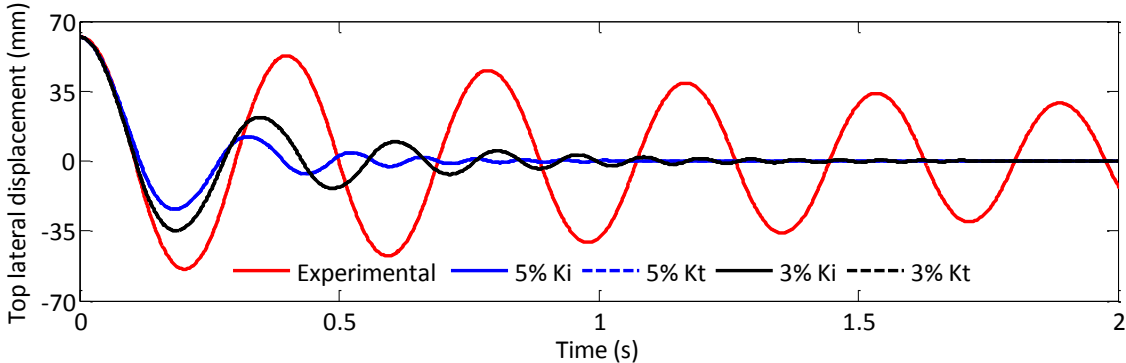


Figure 4: Stiffness proportional damping schemes with the OpenSees multi-spring bed model

It is clear from Figure 3 that the four damping schemes over predict the damping significantly for the lumped plasticity model. Additionally by studying the first 0.5 s of motion, it can be seen that both of the tangent stiffness damping schemes are closer in phase to the experimental result, with both of the schemes resulting in lower damping in comparison to their initial stiffness counterparts. The reason for this is due to the use of initial stiffness proportional damping in combination with nonlinear force-displacement behaviour, which is observed in Figure 2. When the chosen damping is initial stiffness proportional and there is a low post-yield stiffness the fractions of damping within the model increase with a decrease in stiffness (Carr 2004). This is unrealistic for an unbonded post-tensioned precast concrete wall as the contact damping will cause increased damping closer to zero displacement

position. As the 5% and 3% EVD greatly surpasses the required damping for both models they are not appropriate values to use for an isolated unbonded post-tensioned concrete wall, highlighting the significant difference between an isolated wall and a building. Also, it is evident that the peak picking method cannot accurately evaluate the damping in an unbonded post-tensioned concrete wall due to the significant over-prediction observed for the 3% EVD response.

Additionally, from **Error! Reference source not found.** it is clear that the four damping schemes used in the multi-spring bed macro model also over predict the damping. For the OpenSees multi-spring bed model the initial stiffness and tangent stiffness matrices are equal, leading to an identical solution for each level of EVD. Due to the inability to implement the tangent stiffness model in OpenSees, only Ruaumoko was used for the remaining modelling that was conducted.

One of the few pieces of literature found to date that attempted to account for contact damping specifically was Marriott (2009) which has previously been discussed in the introduction to this paper. To implement Marriott's suggested contact damping model, which consists of a linear viscous damper and friction damper, the structure was converted into a single-degree-of-freedom model. Marriott (2009) estimated a total of 2.4% EVD for the specific unbonded post-tensioned concrete wall studied, allocating half or 1.2% EVD (damping co-efficient = 0.971) to each of the linear viscous damper and friction damper (yield force = 0.7865 kN). The viscous damper co-efficient was calculated based on the corresponding secant stiffness at release drift as recommended by Marriot (2009).

O'Hagan et al. (2013) performed a sensitivity analysis on the specimen and test results which are the focus of this paper. Different EVD schemes were implemented using a single degree of freedom that used the experimental force displacement response. By using this experimental force-displacement response and including coulomb friction with a yield force of 0.5 kN (corresponds to 0.64% EVD), optimised ratios for the different stiffness proportional EVD schemes were calculated and found to match well in both phase and amplitude for all schemes. The optimised initial secant stiffness proportional damping ratio found by O'Hagan et al. was 0.775 (damping co-efficient = 0.7543).

Although O'Hagan et al. (2013) investigated a number of different stiffness proportional EVD schemes, the initial secant stiffness proportional method is investigated herein. The initial secant stiffness proportional method is more comparable to Marriott's contact damping method as the viscous damper implemented is also based on the initial secant stiffness. The energy dissipation schemes proposed by Marriott (2009) and O'Hagan et al. (2013) have been implemented using the predictive Ruaumoko lumped plasticity model. Figure 6 shows a comparison of the results of the two aforementioned initial secant stiffness proportional damping schemes versus the experimental free vibration snap back test. Firstly, from Figure 6 it is clear that the free vibration displacement response histories of both models are significantly improved on the 3% and 5% EVD models. As shown in Figure 5 the model proposed by O'Hagan et al. (2013) is more accurate in comparison to the model proposed by Marriott (2009) in terms of displacement amplitude and the overall time it takes for the wall to come to rest. A close up of Figure 5 is shown in Figure 6 for the first 2 seconds of displacement decay. In this time period the model proposed by Marriott (2009) shows a similar response to O'Hagan et al.'s model but over time the increased damping in Marriott's model results in a significant 25 % faster decay. It is expected that O'Hagan et al.'s model is more accurate as it was calibrated specifically for this wall's specifications. Since both models are based on friction damping and viscous damping it appears feasible that both models with fine-tuning would be able to emulate the experimental results. Further analysis will be run to investigate different combinations of friction and viscous damping for both models to yield more accurate results.

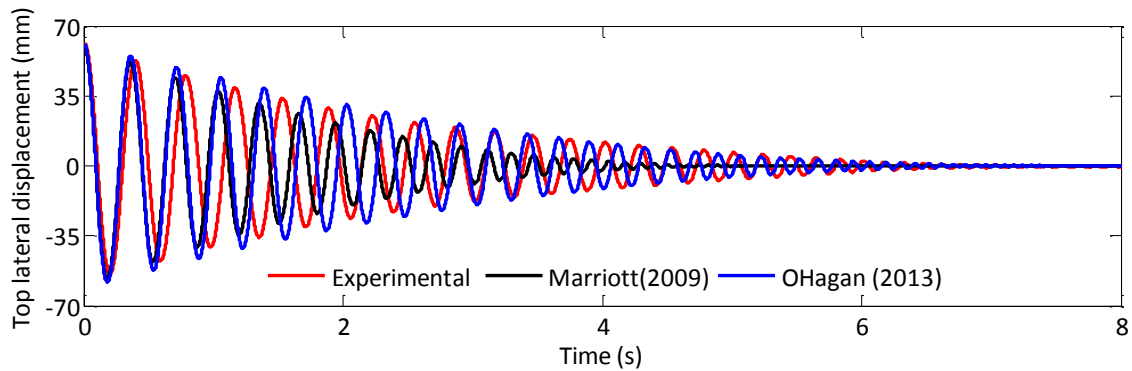


Figure 5: Lumped plasticity model results incorporating damping recommendation proposed by Marriott (2009) and O’Hagan (2013)

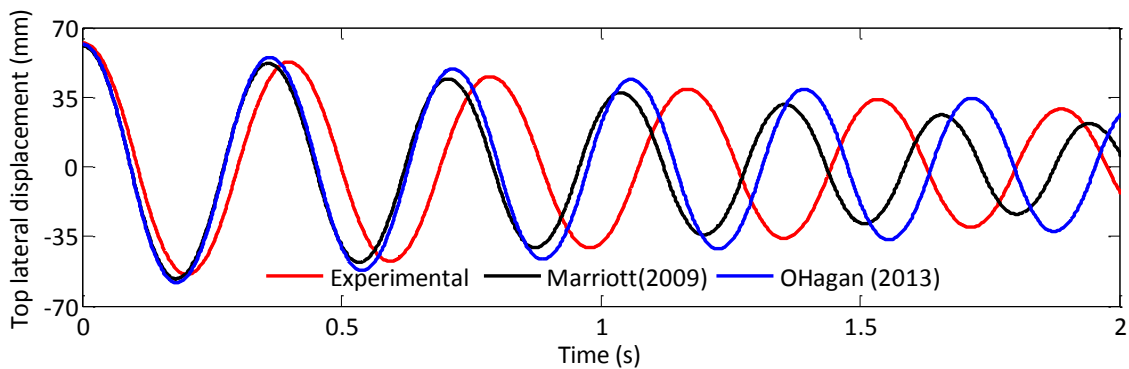


Figure 6: Close up of Figure 5 from 0 to 2 seconds

5 CONCLUSIONS

Both the Ruaumoko lumped plasticity model and the OpenSees multi-spring macro model were able to satisfactorily predict the cyclic response backbone of the wall specimen. The OpenSees multi-spring macro model is more complex in comparison to the Ruaumoko lumped plasticity model, but is able to predict the cyclic response of the wall specimen with increased accuracy. A significant advantage of the multi-spring macro model is that it is a truly predictive model that explicitly accounts for the rocking interface and prestressing tendons and can incorporate additional elements if required.

The EVD ratio of 3% which previous researchers have used for dynamic time-history analysis of unbonded post-tensioned concrete wall buildings is significantly too high in comparison to the snap back tests performed on an isolated wall in the laboratory, despite the measured experimental EVD being estimated at a similar magnitude of 2.5%. It is important to realise that 3 % EVD may still be valid for an entire building. The combination of friction and viscous damping to represent the damping in an isolated unbonded post-tensioned concrete wall produces promising results. Further analysis is needed to calculate recommended values not only for the wall discussed herein but to be used on varying specifications of unbonded post-tensioned concrete wall.

6 FUTURE WORK

This work begins the process of improving the accuracy of modelling the damping mechanisms associated with unbonded post-tensioned concrete walls. The models discussed here will be used to further investigate various combinations of friction and viscous damping to emulate the test result with increased accuracy. Multiple instantaneous damping mechanisms will also be investigated such as incorporation of the co-efficient of restitution. Further dynamic testing is scheduled, which will include different aspect ratios, additional damping devices and a higher initial post-tensioning force.

7 REFERENCES

- Aaleti, S. and Sritharan, S. (2009). A simplified analysis method for characterizing unbonded post-tensioned precast wall systems. *Engineering Structures* Vol. **31** No. 12: 2966-2975
- Carr, A. J. (2004). "RUAUMOKO users manual.", from www.ruaumoko.co.nz
- Henry, R. S., (2011) Self-centering precast concrete walls for buildings in regions with low to high seismicity. *PhD--Civil Engineering*, University of Auckland. <http://hdl.handle.net/2292/6875>
- Kurama, Y. C., Sause, R., Pessiki, S. and Lu, L. W. (2002). Seismic response evaluation of unbonded post-tensioned precast walls. *ACI Structural Journal* Vol. **99** No. 5: 641-651
- Ma, Q. T. M., (2010) The mechanics of rocking structures subjected to ground motion. *PhD--Civil and Environmental Engineering*, University of Auckland. <http://hdl.handle.net/2292/5861>
- Mander, J. B., Priestley, M. J. N. and Park, R. (1988). THEORETICAL STRESS-STRAIN MODEL FOR CONFINED CONCRETE. *Journal of structural engineering New York, N.Y.* Vol. **114** No. 8: 1804-1826
- Marriott, D., (2009) The Development of High-Performance Post-Tensioned Rocking Systems for the Seismic Design of Structures. Civil Engineering, University of Canterbury Christchurch.
- Mazzoni, S., McKenna, F., Scott, M. H. and Fenves, G. L. (2006) Open System for Earthquake Engineering Simulation. *Pacific Earthquake Engineering Research Center, University of California, Berkeley, California, Ver. 1.7.4.*
- New Zealand Standard 2006. Concrete Structures Standard NZS 3101.
- O'Hagan, J., Twigden, K. M. and Ma, Q. (2013). Sensitivity of post-tensioned concrete wall response to modelling of damping. New Zealand Society for Earthquake Engineering Technical Conference, Wellington, Auckland, April 26-28
- Palermo, A., Pampanin, S. and Marriott, D. (2007). Design, modeling, and experimental response of seismic resistant bridge piers with posttensioned dissipating connections. *Journal of Structural Engineering* Vol. **133** No. 11: 1648-1661
- Pampanin, S., Priestley, M. J. N. and Sritharan, S. (2001). Analytical modelling of the seismic behaviour of precast concrete frames designed with ductile connections. *Journal of Earthquake Engineering* Vol. **5** No. 3: 329-367
- Pennucci, D., Calvi, G. M. and Sullivan, T. J. (2009). Displacement-Based Design of Precast Walls with Additional Dampers. *Journal of Earthquake Engineering* Vol. **13** No. sup1: 40-65
- Perez, F. J., Sause, R. and Pessiki, S. (2007). Analytical and experimental lateral load behavior of unbonded posttensioned precast concrete walls. *Journal of Structural Engineering* Vol. **133** No. 11: 1531-1540
- Priestley, M. J. N., Sritharan, S. S., Conley, J. R. and Pampanin, S. (1999). Preliminary results and conclusions from the PRESSS five-story precast concrete test building. *PCI Journal* Vol. **44** No. 6: 42-67
- Restrepo, J. I. and Rahman, A. (2007). Seismic performance of self-centering structural walls incorporating energy dissipators. *Journal of Structural Engineering* Vol. **133** No. 11: 1560-1570
- Sritharan, S., Aaleti, S., Henry, R. S., Liu, K. Y. and Tsai, K. C. (2008). Introduction to PreWEC ad key results of a proof of concept test. M.J. Nigel Priestley Symposium, North Lake Tahoe, California
- Watkins, J., Henry, R. S. and Sritharan, S. (2013). Analytical modelling of rocking precast concrete walls. Computational Methods in Structural Dynamics and Earthquake Engineering, Kos Island, Greece, 12–14 June 2013